Tissue specificity of fMRI signals at Ultra-high resolution – but where in the tissue?

N. Harel[1], J. Lin[1], Y. Zhang[1], K. Ugurbil[1], E. Yacoub[1]

[1]Center For Magnetic Resonance Research, University of Minnesota, Minneapolis, MN, United States

Introduction

For the past decade, great effort has been put to increasing the spatial resolution and specificity of the fMRI signals from vessel-weighted to more tissue specific signals. The working assumption is that the "tissue" signals mirror changes at the neuronal level. While great progress has been made, the basic and most fundamental questions remain unanswered: where in the tissue do these fMRI "tissue" changes occur? Do they indeed originate at the site of the most active neurons/layer? The aim of this study was to obtain in plane high resolution (150 x 150 μm^2) functional MR images of BOLD (*1*) and contrast-enhanced CBV-weighted (MION) signals (*2*) and correlate them with the underlying cortical laminar cytoarchitectonic organization. Both measurements (fMRI signals and cytoarchitectonic) were obtained within the same animal and cortical section. By obtaining such a correlation, a better understanding of the spatial origin of the fMRI signals was obtained.

Methods

Cats (n=4) were prepared as described previously (*3*). The animals were kept under isoflurane anesthesia throughout the experiment (1% in a N_2O:O_2 mixture of 70:30). Blood pressure, end-tidal CO_2 and body temperature were maintained at normal conditions. Visual stimuli consisted of binocular 30-s high-contrast square-wave moving gratings (0.15 cyc/deg, 2 cyc/s). All MR experiments were performed on a 9.4T/31cm (Oxford, UK) magnet. A single coronal slice perpendicular to area 18 (crossing at Horsley-Clark AP2) was used for the functional study. Anatomic images were obtained using T1-weighted 2D TurboFLASH and 3-D GEMS.

fMRI parameters: Two contrast mechanism were used for the functional studies: BOLD and CBV-weighted (MION). In addition, two imaging sequences were used, Gradient Echo (GE) and Hahn Spin Echo (HSE). Initially, GE and HSE BOLD responses were measured. Next, GE CBV-weighted changes were measured following a bolus injection of MION (10mg Fe/kg). For the GE: Data matrix = 128 x 128, 4 segment EPI, FOV = 2x2 cm^2, yielding a 150 x 150 μm^2 in plane resolution. Slice thickness = 2 mm. TE/TR = 20ms (10ms with MION) /4s. For the BOLD HSE sequence a reduced FOV along the phase encode direction was applied using a selective refocusing pulse. This allowed us to reduce the number of segments needed for the high resolution images. Imaging parameters: FOV: 3.84 x 0.96 cm2 (matrix 256 x 64); Voxel size: 0.15 x 0.15 x 2 mm^3; 2 segments. TE/TR =40ms/4s. Activation maps were overlaid on corresponding anatomical images. The MR signals were cross-correlated with the stimulation paradigm to identify active pixels.

Histology: Following the MR session, the animals were transcardially perfused with 0.1M phosphate buffered saline, followed by a 4% paraformaldhyde (PA) in 0.1M phosphate buffer. The brain was removed and was postfixed in 4% PA. Digital photographs were taken of the intact fixed brain. A 3mm cortical slab (see below) was extracted. The cortical slab was then sectioned with a 15µm slice thickness with a cryostat and was stained with cresyl violet for identification of neuronal distribution. The border between layers was determined based on cytoarchitectonic criteria such as cell types, size and density.

Co-registration: The co-registration of the MR images with the histology preparation was achieved by a multi stage aligning process. Initially, the high quality TurboFlash image corresponding to the functional slice was aligned with a coronal slice of the 3-D GEMS image using BrainVoyager (Brain Innovation, Netherlands). Then, by only adjusting the Z-coordinates, a dorsal (TRA) view was obtained while keeping the coronal functional image plane location market. The TRA image with the market functional slice was then aligned with a photographed dorsal view of the intact brain using visible landmarks (Adobe, Photoshop). Once the exact image plane was determined, a 3mm slab was sectioned and the block underwent histological preparation.

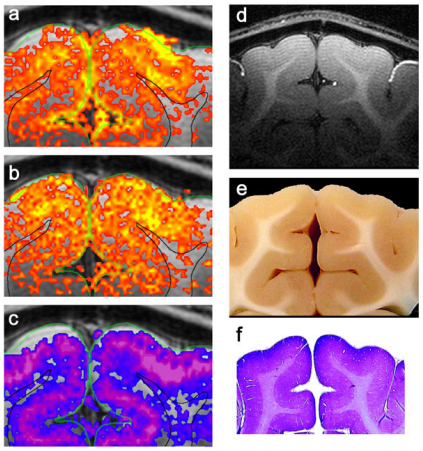

Results

Activation maps were superimposed on high-resolution anatomical images in which the gray and white matter borders were outlined. Panels a-c show GE-BOLD, HSE-BOLD and GE-MION activation maps, respectively. Activation was confined to the primary visual areas (corresponding to Brodmann's areas 17 & 18) and closely followed the gray matter contour. The highest GE-BOLD signal changes were observed at the cortical surface coincides with the large surface vessels. However, in all three maps, spatially defined signal changes were centered over the gray matter region. Following the imaging session, the brain was removed, and the imaged slice was identified (d–e). The cortical slab corresponding to the image plane underwent histological staining (f) and the borders of the cortical layers were identified. The tissue signals were mainly arose from the lower portion of cortical layers II/III and extended down to layer V.

Discussion

In a high resolution fMRI study we have investigated the spatial specificity of the fMRI signals and correlated them with postmortem histochemical slides obtained within the same animal and tissue region. All three fMRI mapping signals show specificity to the middle cortical layers where the majority of orientation selective neurons are found. Thus, the tissue signals were found to be spatially correlated with cortical functional laminar architecture. However, the largest GE-BOLD signal changes were observed at the cortical surface apparently from large cortical vessels. The enhanced sensitivity of the MION signal (*2, 4*), even at 9.4T, allowed us to more clearly resolve signals from deeper areas. While a vascular filter function and MION dose dependence (5) could affect the spaitial pattern of the MION map, the specificity of the signal to the middle layers is supported by the similar pattern observed in the BOLD maps free from these methodological constrains.

Acknowledgements: Supported by the WM KECK Foundation and NIH P41 RR08079 and R21 EB00565.

References: 1) Ogawa et al., *PNAS* 1990.; 2) Mandeville *et al., MRM 1998;* van Bruggen et al., *JCBFM* 1998; Kennan et al., *MRM* 1998.; 3) Harel et al., *JCBFM* 2002.; 4) Mandeville *et al., MRM*, 2001; Vanduffel et al., *Neuron* 2001.; 5) Mandeville & Marota, *MRM* 1999.